

Finite Element Based Durability Assessment of a Free Piston Linear Engine Component

M. M. Rahman¹, A. K. Ariffin¹, S. Abdullah¹ and N. Jamaludin¹

Abstract: A modern computational approach based on finite element analysis for durability assessment in a two-stroke free piston linear engine component using the variable amplitude loadings is presented. This paper describes the finite element analysis techniques to predict the fatigue life and identify the critical locations of the component. The effect of mean stress on the fatigue life is also investigated. The finite element modeling and analysis has been performed using a computer-aided design and a finite element analysis software package, and the fatigue life prediction was carried out using finite element based fatigue life prediction codes. The fatigue crack initiation approach was utilizing to assess the durability of the component of the free piston linear engine. The acquired results utilizing the crack initiation approach indicate that when the loading sequences is predominantly tensile in nature (such as SAETRN loading), the SWT and the Morrow models give shorter life than that obtained using the Coffin-Manson model. However, the Coffin-Manson method gives conservative prediction when the time histories are predominantly compressive (SAESUS loading), and zero mean stress loadings (SAEBKT loading). The results are capable of showing the contour plots of the fatigue life histogram and damage histogram at the most critical location.

Keyword: Durability, fatigue life, finite element, free piston linear engine.

1 Introduction

A two-stroke free piston linear generator (LG) engine consists of a combustion engine and a linear electrical machine into a single unit without a crankshaft. This provides an unconventional solution for series hybrid vehicles and distributes power units [Arshad, Sadarangani, Bäckström, Thelin (2002), Cosic, Lindbäck, Arshad, Leksell, Thelin, Nordlund (2003), Arshad, Thelin Bäckström, Sadarangani (2004)]. The free piston engine consists of a double-ended piston, double-ended cylinder, and a liner alternator. The piston is enclosed inside the double-ended cylinder where it moves freely along the cylinder's axis. The combustion of a premixed fuel-air charge occurs successively at opposite ends of the cylinder creating the driving force for piston oscillation. Magnets are fixed on the piston so that their oscillating motion creates a varying magnetic flux within the alternator core. The alternator converts this changing flux into electricity, directly harnessing the mechanical work of the piston as electrical power. The dynamics of the piston are moderated by the linear alternator which controls the electromagnetic force on the piston. The alternator precisely manages the piston's kinetic energy so that the desired compression ratio is reached on each piston stroke [Van Blarigan (1998)]. The schematic diagram of a two-stroke free piston linear generator engine is shown in Fig. 1.

Most of the previous studies [Van Blarigan (1998), Cosic, Lindbäck, Arshad, Leksell, Thelin, Nordlund (2003), Arshad, Thelin Bäckström, Sadarangani (2004), Aichlmayr (2002)] related to the LG engine utilizes two combustion chamber in order to get the linear movement of the piston. For this linear engine, crank and camshaft will not be required and there was no rotary move-

¹ Computational and Experimental Mechanics Group, Department of Mechanical and Materials Engineering, Universiti Kebangsaan Malaysia. 43600 UKM, Bangi, Selangor DE, Malaysia. Phone:+6(03)89216012; Fax: +6(03)89216040 E-mail: mustafiz@eng.ukm.my

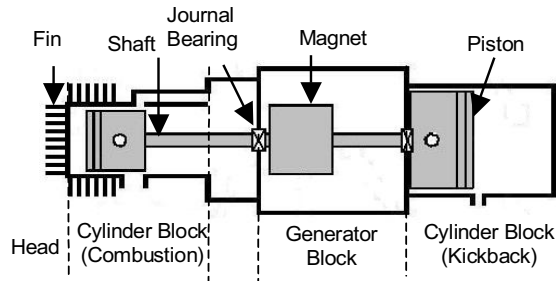


Figure 1: A two-stroke free piston linear generator engine

ment involved. In addition, the linear system of the engine should prove to be more efficient as the frictional losses associated with the crank and rod bearings are not present. However, the previous study [Aichlmayr (2002)] used a single piston engine with rebound device and the system tended to create unbalanced situation. These need to be encountered for this new free piston linear engine.

Durability is one of the most important design requirements that are essential for a new engine product to achieve successful market competitiveness. For the vehicle body structure the durability assessment has traditionally been performed at the later part of the product development stage when prototypes are available and heavily relied upon the result of the ground durability tests. This process is very time consuming and often results in over-design with weight penalties, which is the major obstacle to achieve fuel economy. Due to the development in the computer-aided engineering (CAE) tools, a three-step process that includes multibody dynamic analysis, finite element analysis, and fatigue life prediction, is widely used today for early product durability evaluation [Brek, Stephens, Dopker (1993), Kuo, Kelkar (1995), Yim, Lee (1996)]. This approach helps the designer to acquire the necessary information for continuous design analysis, and predicts the durability of the free piston linear generator engine in the early design stage, thereby eliminating some of the shortcomings in the traditional durability evaluation method.

The durability of the engine structure has increasingly become the vital issues due to the multi-

disciplinary research problem that involves the multibody dynamics, structural analysis and fatigue life prediction. Moreover, due to the requirement of the peak-valley editing and rainflow counting procedure in the fatigue life prediction, an analytical relationship between the dynamic stress and the fatigue life can not be obtained easily. Thus it becomes really difficult, if not impossible, to obtain the fatigue life design analytically. The objectives of this paper are to predict the fatigue life of a free piston linear engine cylinder block using nominal stress-life, normal strain-life fatigue prediction methods and also to investigate the effect of mean stress on the fatigue life.

2 Proposed Durability Analysis

Durability analysis can be used to determine how long a component can survive in a given service environment. In a general case the durability refers to the ability of a component to function in the presence of defects for a given environment/loading. In practice, however, the predominant failure mode is fatigue and hence, the term durability analysis was used to describe the analysis of a fatigue performance.

Fatigue analysis has traditionally been performed at a later stage of the design cycle. This is due to the fact that the loading information could only be derived from the direct measurements, which require a prototype [Bannantine, Comer, Handrock (1990), Stephens, Fatemi, Stephens, Fuchs (2001)]. Multibody dynamics (MBD) [Kim, Kim (2002)] is capable of predicting the component loads which enable the designer to undertake a durability assessment even before a prototype is fabricated. The purpose of analysing a structure early in the design cycle is to reduce the development time and cost. This is achieved by determining the critical regions of a structure and improving the design before prototypes are built and tested. Three computational processes are utilized to perform the durability analysis using CAE tools. The processes of the durability assessment are as follows:

- (i) Multibody dynamic simulation – to determine the loading on a component based on

system inputs;

- (ii) Finite element analysis (FEA) – to determine the stress/strain state of a component for a given load condition;
- (iii) Fatigue analysis – to calculate the fatigue life for the component of interest and identify the critical locations.

The fatigue analysis is used to compute the fatigue life at a single location in a structure. For multiple locations the process is repeated using geometry information applicable for each location. The required inputs for the fatigue analysis process are shown in Fig. 2. The three input information are descriptions of the material properties, loading histories and geometry. The details of these inputs are as follows.

- (i) Material information – cyclic or repeated material data based on a constant amplitude testing.
- (ii) Load histories information – measured or simulated load histories applied to a component. The term “loads” is used to represent forces, displacements, accelerations, etc.
- (iii) Geometry information – relates the applied load histories to the local stresses and strains at the location of interest. The local stresses and strains information are usually derived from the FE results.

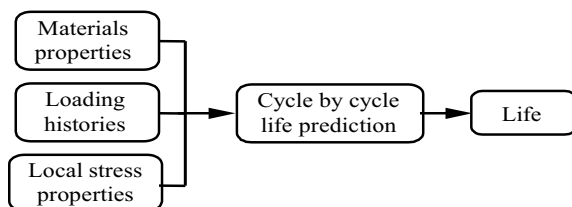


Figure 2: Schematic diagram of fatigue life estimation

The FE based durability analysis can be considered as a complete engineering analysis for the components. The fatigue life can be estimated for

every element in the finite element model, and the contour plots of life or damage can be obtained. The geometry information is provided by the FE results for each load case applied independently. Appropriate material properties are also provided for the desired fatigue analysis method. An integrated approach to durability analysis combines the multibody dynamic analysis, finite element analysis, and the fatigue analysis into a consistent entity for the prediction of the durability of a component. The process of finite element based integrated durability analysis is shown in Fig. 3.

3 Fatigue Analysis Methods

Fatigue analyses can be performed using either one of the three basic methodologies including the stress-life approach, crack initiation (strain-life) approach, and crack propagation (crack growth) approach. The stress-life method was first applied over a hundred years ago [Wöhler (1867)] and considers nominal elastic stresses and how they are related to life. This approach to the fatigue analysis of components works well for situations in which only elastic stresses and strains are present. However, most components may appear to have nominally cyclic elastic stresses but stress concentrations present in the component may result in local cyclic plastic deformation. Under these conditions, the local strain-life method uses the local strains as the governing fatigue parameter. The fatigue crack initiation or strain-life approach can be used proactively for a component during early design stages. Fatigue life estimates may be applied for various potential design geometries and manufacturing processes prior to the existence of any actual components provided the material properties are available. This approach reduced the number of design iterations by identifying and rejecting unsatisfactory designs early in the design process. Therefore, the design cycle is shortened and the final can products reach the market quickly. The local strain-life approach is preferred if the loading history is irregular and where the mean stress and the load sequence effects are thought to be of importance. Crack propagation or linear elastic fracture mechanics (LEFM) approach is used to predict how quickly

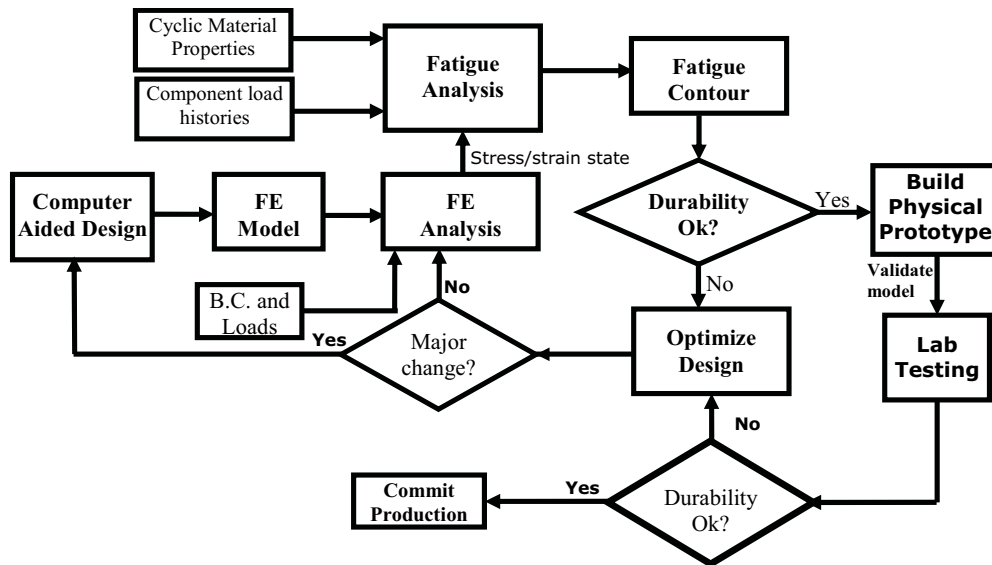


Figure 3: The finite element based durability analysis

pre-existing cracks grow and also to estimate how many loading cycles are required to cause the cracks to reach a critical size when catastrophic failure would occur.

The crack initiation approach involves the techniques for converting the loading history, geometry and materials properties (monotonic and cyclic) input into a fatigue life prediction. The operations involved in the prediction process must be performed sequentially. First, the stress and strain at the critical region are estimated and then the rainflow cycle counting method [Matsuishi, Endo (1968)] is used to reduce the load-time history. The next step is to use the finite element method to convert the reduced load-time history into a strain-time history and also to calculate the stress and strain in the highly stressed area. Then, the crack initiation methods are employed to predict the fatigue life. The simple linear hypothesis proposed by Palmgren (1924) and Miner (1945) is used to accumulate the fatigue damage. Finally, the damage values for all cycles are summed until a critical damage sum (failure criteria) is reached. The fatigue resistance of metals can be characterized by a strain-life curve. These curves are derived from the polished laboratory specimens tested under completely reversed strain control. The relationship between the total strain amplitude ($\Delta\epsilon/2$) and the reversals to failure ($2N_f$) can

be expressed in Eq. (1) [Coffin (1964), Manson (1953)]. The Coffin-Manson total strain-life is mathematically defined as in Eq. (1).

$$\frac{\Delta\epsilon}{2} = \frac{\sigma'_f}{E} (2N_f)^b + \epsilon'_f (2N_f)^c \quad (1)$$

where N_f is the fatigue life; σ'_f is the fatigue strength coefficient; E is the modulus of elasticity; b is the fatigue strength exponent; ϵ'_f is the fatigue ductility coefficient; and c is the fatigue ductility exponent. The typical strain-life curves based on Coffin-Manson relationship are shown in Fig. 4.

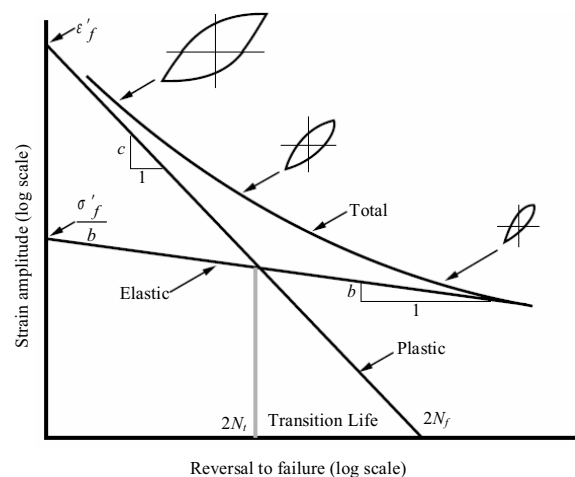


Figure 4: The typical strain-life curve

In designing for the durability, the presence of nonzero mean stress normal stress can influence fatigue behaviour of materials due to a tensile or compressive normal mean stress. In conjunction with the local strain-life approach, many models have proposed to quantify the effect of mean stresses on fatigue behaviour. The commonly used models in the ground vehicle industry are those by Morrow (1968) and by Smith, Watson, and Topper (1970). These two models are described in the following sections.

[Morrow (1968)] has proposed the following relationship when a mean stress is expressed in Eq. (2).

$$\varepsilon_a = \frac{\sigma'_f - \sigma_m}{E} (2N_f)^b + \varepsilon'_f (2N_f)^c \quad (2)$$

The Eq. (2) implies that the mean normal stress taken into account by modifying the elastic part of the strain-life curve by the mean stress (σ_m). Morrow's mean stress correction model is shown in Fig. 5.

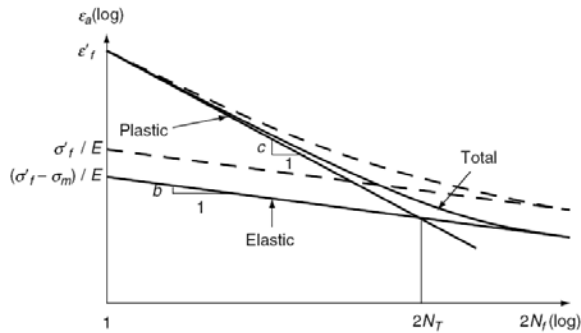


Figure 5: Morrow's mean stress correction model

[Smith, Watson, and Topper (1970)] proposed another mean stress model which is called Smith-Watson-Topper (SWT) mean stress correction. It is mathematically defined in Eq. (3).

$$\sigma_{\max} \varepsilon_a E = (\sigma'_f)^2 (2N_f)^{2b} + \sigma'_f \varepsilon'_f E (2N_f)^{b+c} \quad (3)$$

where σ_{\max} is the maximum stress, and ε_a is the strain amplitude.

The Neuber method is used to estimate elastic-plastic stresses and strains at the roots of notches

on the basis of elastic stress analysis. It applies where the yielding is limited in extent; under these circumstances it provides a reasonable approximation for the redistribution of stress and strain. When yielding is more widespread, for instance when the loads are very high, or notches very shallow (or absent) it may give non-conservative predictions. Graphical solution using the Neuber's rule is shown in Fig. 6, where K_e , K_σ and K_T represent the strain, stress and theoretical stress concentration factor respectively. Neuber's hypothesis assumes that the product of two concentration factors (K_e and K_σ) stays constant until yielding starts at the notch. Upon yielding, the local stress and local strain are no longer linearly related and the local values are related in terms of K_e and K_σ . After yielding occurs the local stress concentration factor decreases with respect to K_T and the strain concentration factor increases with respect to K_T .

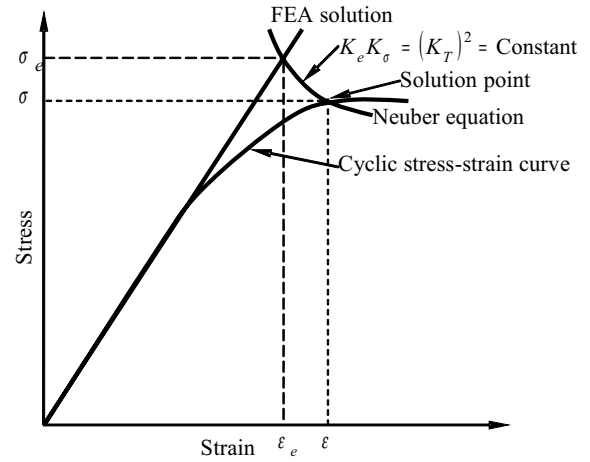


Figure 6: Graphical solution using the Neuber's rule

Plasticity is accounted for the crack initiation method by the Neuber method. The elastic stresses and strains are identified on the elastic line and then corrected to fall onto the cyclic stress-strain curve to determine the elastic-plastic stresses and strains. This elastic-plastic strain is used to identify damage on the strain-life damage curve. Neuber's elastic-plastic correction sometimes called a notch correction is based on the simple principle that the product of the elas-

tic stress and strain should be equal to the product of the elastic-plastic stress and strain from the cyclic stress-strain curve. Then through an iterative method, the elastic-plastic stress and strain can be determined. Neuber's rule is used to calculate elastic-plastic stress and strain from their wholly elastic theoretical equivalents by an elastic finite element analysis. So that with K_T is taken as unity, i.e. the local elastic finite element stresses and strains can be expressed as Eq. (4).

$$\varepsilon_e \sigma_e = \varepsilon \sigma = \text{constant} \quad (4)$$

Both ε and σ can be calculated from Eq. (4) together with the equations for the cyclic stress-strain curve and the twice the cyclic-stress strain curve.

4 Material Information

Materials model and material properties play an important role in the results of the FE method. The material properties is one of the major input which is the definition of how a material behaves under the cyclic loading conditions. The cyclic material properties are used to calculate the elastic-plastic stress-strain response and the rate at which fatigue damage accumulates due to each fatigue cycle. The materials parameters required depend on the analysis methodology being used. Normally, these parameters are measured experimentally and available in various handbooks [Juvinal, Marshek (1991), Lipton and Juvinal (1963), Reemsnyder (1985)]. Two different materials were used for the cylinder block of the free piston engine, AA5083-87-CF and AA6061-T6-80-HF. Their characteristics are discussed in the following sections. The mechanical properties of the two aluminum alloys are tabulated in Table 1.

Figures 7 and 8 represent the cyclic and monotonic stress-strain curves for the AA5083-87-CF and AA6061-T6-80-HF respectively. The figures show how these two materials behave under cyclic loading conditions and how they behave relative to one another. It can be seen that both the materials cyclic yield strength is higher than that of monotonic yield strength. This implies that both

the materials are stronger under cyclic loading i.e. cyclic hardening or strain hardening.

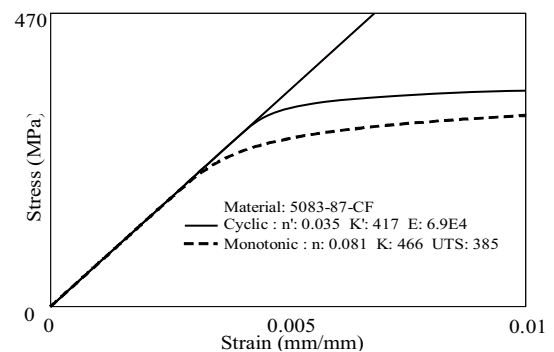


Figure 7: Cyclic and monotonic stress-strain curves of AA5083-87-CF

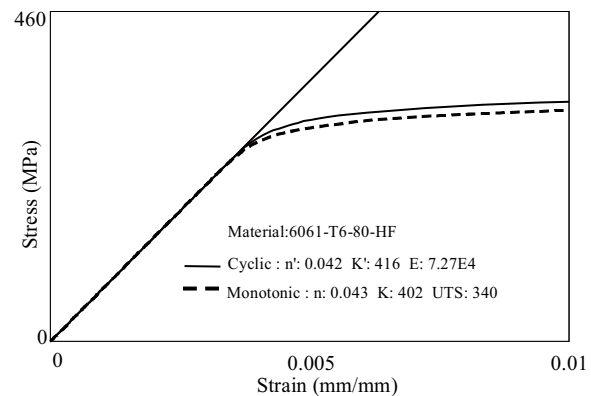


Figure 8: Cyclic and monotonic stress-strain curves of AA6061-T6-80-HF

Fig. 9 represents the strain-life curves for both materials. The figure clearly shows that the materials have different fatigue life behaviour. Fig. 9 is plotted based on the SWT relationship. From the figure, it can be seen that the differences in the figure life behaviour is significant in the short life (low cycle fatigue). On the other hand, the differences becomes less significant in the long life are (high cycle fatigue).

5 Loading Information

Loading is another major input to the finite element based fatigue analysis. Loading information can be obtained using a number of different methods. Local or nominal strains can be measured

Table 1: Mechanical properties of the two aluminum alloys

Properties	Aluminum Alloy	
	AA5083-87-CF	AA6061-T6-80-HF
Monotonic Properties		
Modulus of elasticity, E (GPa)	69.0	72.7
Yield Strength, YS (MPa)	285	313
Ultimate strength, S_u (MPa)	385	340
Strength Coefficient, K (MPa)	466	402
Strain hardening exponent, n	0.081	0.043
Fracture toughness, K_{1C} (MPa-m ^{1/2})	43	29
Cyclic and fatigue Properties		
Fatigue strength coefficient, σ'_f (MPa)	650	645
Cyclic strength coefficient, K' (MPa)	417	416
Cyclic strain hardening exponent, n'	0.035	0.042
Fatigue strength exponent, b	-0.094	-0.097
Fatigue ductility coefficient, ϵ'_f	2.26	0.22
Fatigue ductility exponent, c	-1.01	-0.6
Fatigue limit, $S_f@2 \times 10^8$ cycles (MPa)	133.85	126.29

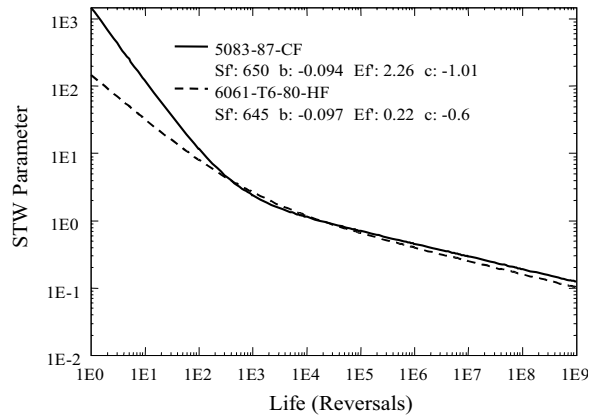


Figure 9: Smith-Watson-Topper life curve of 5083-87-CF and 6061-T6-80-HF

by means of strain gages. Nominal loads can be measured through the use of load cells or more recently they can be derived externally by means of analysis. Since early methodologies relied on measurement from the physical components, the application of the fatigue analysis methods has been confined to the analysis of service failures or at best to the latter stages of the design cycle where the components and systems first become available. The ability to predict component loads analytically means that the physical components are no longer a prerequisite for the durability anal-

ysis. Thus the analysis can proceed much earlier in the design cycle. It is important to note that, in this context the loading is defined as the set of phase-relating sequences such as time histories that uniquely map the cyclic loads to each external input location on the component.

Several types of variable amplitude loading history were selected from the SAE and ASTM profiles. It is important to emphasize that these sequences are not intended to represent standard loading spectrum in the same way that Carlos or Falstaf was performed. However, they do contain many features which are typical of the automotive industries applications and therefore are useful in the evaluation of the life estimation methods. The component was loaded with three random time histories corresponding to typical histories for transmission, suspension and bracket components at different load levels. The first load history has a predominantly tensile (positive) mean which reflects sudden changes in mean that is referred to as the transmission history. The second load history has a predominantly compressive (negative) mean that is referred as suspension history. The third load history representing a vibration with nearly zero mean loads which is referred as the bracket history. The detailed information about these histories can be referred in the liter-

ature [Tucker and Bussa (1977)]. These histories were scaled to two peak strain levels and used as full-length histories. In addition, a random history including many spikes was selected for the simulation of spike removal. The variable amplitude load-time histories are shown in Fig. 10. The terms of SAETRN, SAESUS, and SAEBKT represent the load-time history for the transmission, suspension and bracket respectively. The considered load-time histories are based on the SAE's profile. The abscissa is the time, in seconds.

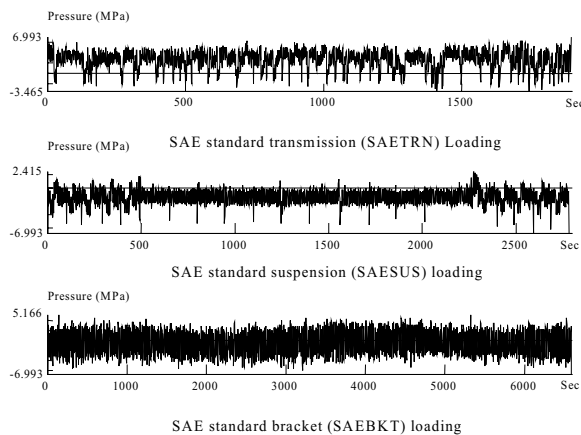


Figure 10: The variable amplitude load-time histories

The realistic loading time histories are often difficult to obtain. A measurement of these is required during typical and extreme operating conditions. This is normally carried out by a dedicated measurement device such as transducers and data acquisition equipment. The loading information usually requires a measurement to instrument and collect the required load time histories under realistic conditions. It is also normal to test a product in fatigue prior to releasing to market. The finite element based durability analysis helps to eliminate unnecessary tests by allowing the engineer to check out the fatigue performance analytically and to optimize the selection of the material, manufacturing processes, and geometry, within the constraints of total cost and loading environment. Carrying out this optimization analytically, rather than by testing, can shorten the time to market and reduce costs significantly.

6 Numerical Example

A geometric model of the cylinder block of the free piston engine is considered in this study. There are several contact areas including cylinder head, gasket and hole for bolt. Therefore, constraints are employed for the following purposes: (i) to specify the prescribed enforce displacements, (ii) to simulate the continuous behavior of displacement in the interface area, (iii) to enforce rest condition in the specified directions at grid points of reaction. Three-dimensional model of free piston linear engine cylinder block was developed using CATIA[®] software. A parabolic tetrahedral element was used for the solid mesh. Sensitivity analysis was performed to obtain the optimum element size. These analyses were performed iteratively at different element lengths until the solution obtained appropriate accuracy. Convergence of the stresses was observed as the mesh size was successively refined. The element size of 0.20 mm was finally considered. A total of 35415 elements and 66209 nodes were generated with 0.20 mm element length. A pressure of 7.0 MPa was applied on the surface of the cylinder head chamber generating a compressive load. A pressure of 0.3 MPa was applied on the bolt-hole surface generating a preload. In addition, 0.3 MPa pressure was applied on the gasket surface.

The Multi-point Constraints (MPCs) [Schaeffer (2001)] were applied on the bolt - hole for all six degree of freedom and were used to connect the parts through the interface nodes. These MPCs were acting as an artificial bolt and nut that connect each parts of the structure. Each MPC's will be connected using a Rigid Body Element (RBE) that indicates the independent and dependent nodes. The configuration of the engine is constrained by bolting the cylinder head and the cylinder block. In the condition with no loading configuration, the RBE element with six-degrees of freedom were assigned to the bolts and the hole on the cylinder head. The independent node was created on the cylinder block hole. Due to the complexity of the geometry and loading on the cylinder block, a three-dimensional FEM was adopted as shown in Fig. 11. The loading and constraints on the cylinder block are shown in Fig.

12.

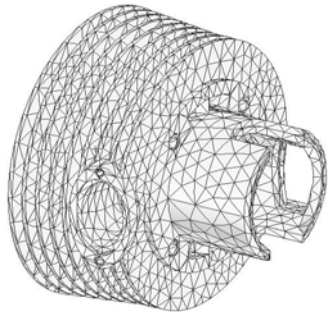


Figure 11: Three-dimensional finite element model

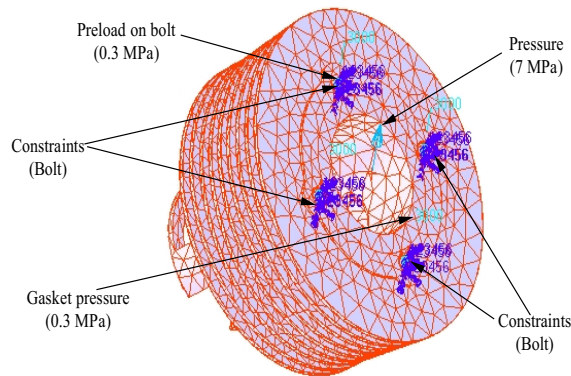


Figure 12: The loading, boundary conditions and constraints

The linear static finite element analysis was performed using MSC.NASTRAN[®] finite element software. The bolt - holes areas were found to experience the highest stresses. The maximum principal stresses and strains are used for the subsequent fatigue life analysis and comparisons. The maximum principal stresses distribution of cylinder block for the linear static analysis is presented in Fig. 13. From the acquired results, the maximum principal stress of 23.4 MPa occurring at node 92190 was obtained. The fatigue life of the cylinder block is predicted using variable amplitude loading conditions (see Fig. 10). The predicted fatigue life results of the cylinder block corresponding to 99.6% reliability value are shown in Fig. 14. From the results, it is shown

that the predicted fatigue life of the AA6061-T6-80-HF aluminum alloy at the most critical location, near the bolt-hole edge (node 92190), is $10^{3.44}$ seconds using the Coffin-Manson method. The fatigue life is represented in terms of seconds using the variable amplitude SAESUS loading histories. The fatigue equivalent unit is 3000 cpm (cycle per min) of the time history. The critical locations are shown in Fig. 14 using the SAESUS loading histories. It is found that the bolt - hole edge is the most critical positions for the cylinder block.

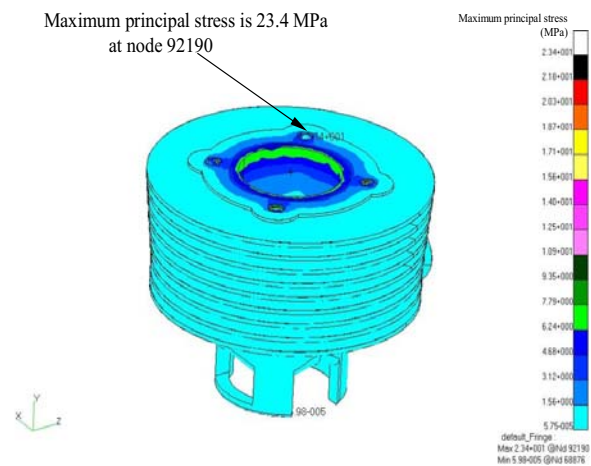


Figure 13: The maximum principal stresses distribution

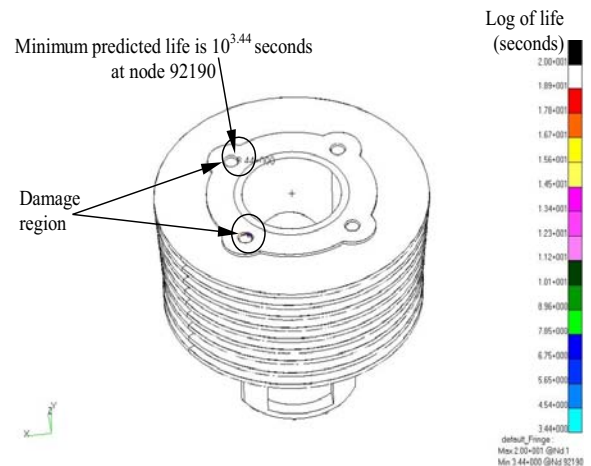


Figure 14: Predicted Fatigue log of life contour for SAESUS loading conditions

Table 2: Predicted fatigue life at most damage location (node 92190).

Loading conditions	Predicted fatigue life in hours					
	AA5083-87-CF			AA6061-T6-80-HF		
	SWT	Morrow	Coffin-Manson	SWT	Morrow	Coffin-Manson
SAETRN	9.73×10^4	2.31×10^5	4.80×10^5	2.87×10^5	7.05×10^5	1.57×10^6
SAESUS	6.36×10^3	7.36×10^3	5.47×10^3	1.68×10^4	1.17×10^4	5.62×10^3
SAEBKT	3.60×10^3	3.38×10^3	2.98×10^3	1.02×10^4	9.48×10^3	8.97×10^3

Most realistic service situations involve nonzero mean stresses. It is, therefore, vital to know the influence of the mean stress on the fatigue process with the fully reversed (zero mean stress) laboratory data normally employed in the assessment of real situations. Two mean stress correction methods are considered in this study including the SWT and the Morrow mean stress correction methods. It is difficult to categorically select one procedure the preference to the other. The predicted fatigue life at most critical location using different loading histories are tabulated in Table 2. It is observed that when using the loading sequences which predominantly tensile in nature (SAETRN loading), the SWT, and the Morrow methods give shorter life than that results obtained by the Coffin-Manson model. However, for the predominantly compressive loading (SAESUS), particularly for wholly compressive cycles, the SWT, and the Morrow's methods are found to give longer life than the Coffin-Manson model. When using the time history roughly zero mean loading (SAEBKT), all the three methods give approximately similar results. Table 3 summarised the results of the fatigue predicted life using the SAESUS loading conditions for the different aluminum alloys. From Table 3, it is also observed that the predominantly tensile (positive) mean loading produces longer life than the compressive mean loading (SAESUS). It shows that the AA7175-T73 alloy is the most superior material having with the longest life among the aluminum alloys while the AA4032-T6 is found to be the weakest material. In designing for durability, the presence of a nonzero mean stress can influence the fatigue behaviour of materials because a tensile or a compressive mean stress has been shown to be responsible for accelerating or de-

celerating crack initiation. It is observed that the compressive mean stresses are beneficial while the tensile mean stresses are detrimental to the fatigue life. This phenomenon is dominant when the mean stress levels are relatively low compared to the cyclic yield stress and the fatigue behaviour falls in the long-life regime where elastic strain is dominant.

The three-dimensional cycle histogram and corresponding damage histogram for the AA6061-T6-80-HF aluminum alloy using SAESUS loading histories are shown in Fig. 15 and Fig.16 respectively. Fig. 15 shows the results of the rainflow cycle count for the critical location on the component. It is observed that there are a lot of cycles at the low stress range. However, the cycles significantly decrease at the high stress range. The height of each tower represents the number of cycles at that particular stress range and mean. Fig. 16 indicates that the lower stress ranges produced zero damage. The figure also shows that most of the damages are found to occur at the high stress ranges. The damages at the higher ranges are found to be widely distributed which means that it cannot point to a single event causing damage.

Local single location fatigue analysis usually comes in the forms of a histogram of rainflow range cycles or damage [Bishop, Sherratt (2000)]. Joint plot of cycle histogram and corresponding damage histogram for the AA6161-T6 using the SAESUS loading histories is shown in Fig. 17. The figure shows both the results of the rainflow cycle count and the damage for the critical location on the component. It is also observed that the lower stress ranges produced zero damage. All the damage is observed to be generated from the

Table 3: Predicted fatigue life for different aluminum alloys at most damage location using the SAESUS loading histories

Materials (Aluminum alloys)	Predicted life in hours		
	SWT	Morrow	Coffin-Manson
AA2014-T6	1.53×10^5	2.59×10^4	1.01×10^4
AA2024-T6	2.28×10^4	1.03×10^4	4.61×10^3
AA2024-T86	4.27×10^5	8.34×10^4	2.55×10^4
AA2048	9.62×10^4	3.02×10^4	1.09×10^4
AA2090-T86	5.72×10^5	1.01×10^5	3.01×10^4
AA4032-T6	2.19×10^3	1.46×10^3	949
AA5083-87	1.68×10^4	1.17×10^4	5.62×10^3
AA5454	5.44×10^3	6.37×10^3	5.04×10^3
AA6009-T9	5.42×10^3	3.52×10^3	2.22×10^3
AA6053-T6	2.90×10^4	1.44×10^4	6.95×10^3
AA6061-T6	1.68×10^4	1.17×10^4	5.62×10^3
AA6069-T6	7.09×10^4	2.42×10^4	9.13×10^3
AA6151-T6	4.05×10^3	2.73×10^3	1.80×10^3
AA6262-T9	3.67×10^4	1.74×10^4	8.06×10^3
AA6061-T6	6.36×10^3	7.36×10^3	5.47×10^3
AA7075-T6	3.24×10^6	2.95×10^5	7.88×10^4
AA7175-T73	4.80×10^6	5.87×10^5	8.71×10^4

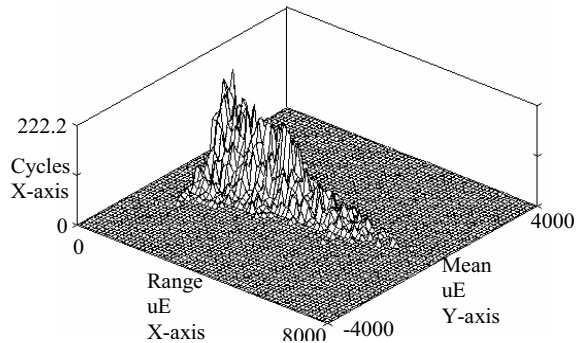


Figure 15: The cycle histogram of critical location for AA6061-T6-80-HF

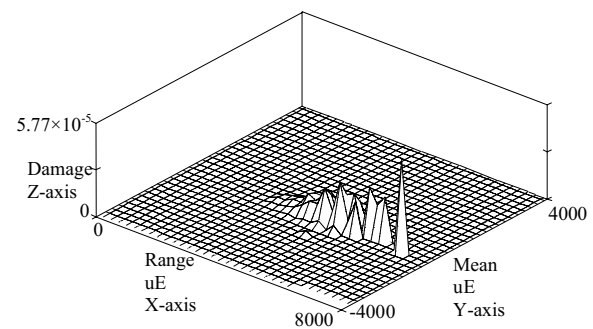


Figure 16: The damage histogram of critical location for AA6061-T6-80-HF

cycles in the higher stress range, which would be expected.

7 Conclusion

A computational approach of the fatigue analysis methodology for the life prediction is presented. Based on the conducted study, several conclusions can be drawn with regard to the fatigue life prediction of a two-stroke free piston engine when subjected to variable amplitude load-

ing conditions. The obtained results indicate that the influences of mean stress are different for the compressive and the tensile mean stress. The predicted fatigue life appears to be more conservative for the tensile mean stress than the compressive mean stress. In designing for durability, the presence of a nonzero mean stress can influence fatigue behaviour of materials because a tensile or a compressive mean stress has been shown to be responsible for accelerating or decelerating the crack initiation process. It is concluded that the

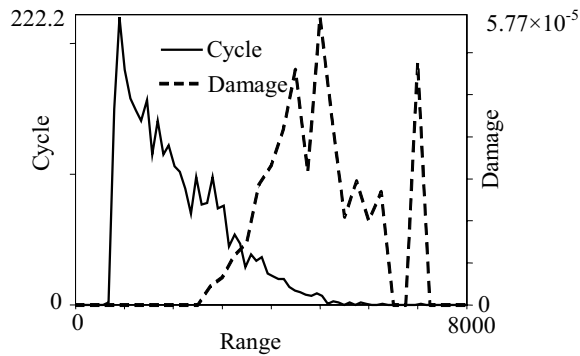


Figure 17: Combined plot of histogram of damage and rainflow range cycles

compressive mean stresses are found to be beneficial and tensile mean stresses are detrimental to the fatigue life. The durability assessment results are significant to improve the component design at the early developing stage. The results are capable of determining the premature products failure phenomena. The proposed approach can be used an efficient and reliable means for the durability assessment of a prototype engine with actual service environments in the early developing stage.

Acknowledgement: The authors would like to thank the Department of Mechanical and Materials Engineering, Universiti Kebangsaan Malaysia. The authors are also grateful to the Ministry of Science, Technology and Innovation, Malaysia under IRPA project (No: 03-02-02-0056 PR0025/04-03) for providing financial support.

References

Aichlmayr, H.T. (2002): *Design Consideration Modeling, and Analysis of Micro-Homogeneous Charge Ignition Combustion Free-Piston Engine*. PhD Thesis Dissertation. University of Minnesota, USA.

Arshad, W.M.; Sadarangani, C.; Bäckström, T.; Thelin, P. (2002): Finding an Appropriate Electrical Machine for a Free Piston Engine Generator. *Proceedings of the 19th International Battery, Hybrid and Fuelcell Electrical Vehicle Symposium (EVS-19)*, Busan, Korea, pp. 427-438.

Arshad, W.M.; Thelin, P.; Bäckström,

T.; Sadarangani, C. (2004): Use of Transverse Flux Machines in a Free Piston Generator. *IEEE Transactions on Industry Applications*, vol. 40, no. 4, pp. 1092-1100.

Bannantine, S.A.; Comer, J.J.; Handrock, J.L. (1990): *Fundamentals of Metal Fatigue Analysis*. New Jersey, USA: Prentice-Hall.

Bishop, N.W.M.; Sherratt, F. (2000): *Finite Element Based Fatigue Calculations*. Kilbride, Glasgow: NAFEMS Ltd.

Brek, W.K.; Stephens, R.I.; Dopker, B. (1993): Integrated Computational Durability Analysis. *ASME J. of Engineering for Industry*, Vol. 115, no. 4, pp. 492-497.

Coffin L. F. Jr. (1964): A Study of the Effects of Cyclic Thermal Stresses on a Ductile Metal. *ASME Transactions*, vol. 76, pp. 931-950.

Cosic, A.; Lindbäck, J.; Arshad, W.M.; Leksell, M.; Thelin, P.; Nordlund, E. (2003): Application of a Free Piston Generator in a Series Hybrid Vehicles. *Proceedings of the 4th International Symposium on Linear Drives for Industrial Applications (LDIA 2003)*, Birmingham, England, pp. 541-544.

Juvinall, R.C.; Marshek, K.M. (1991): *Fundamentals of Machine Component Design*, New York : John Wiley and sons.

Kim, H.S.; Kim, C.B. (2002): Flexible Multi-body Dynamic Analysis using Reduced Deformation Modes. *Proceedings of the First Asian Conference on Multibody Dynamics*, Iwaki, Japan, No. T313, pp. 201-208.

Kuo, E.Y.; Kelkar, S.G. (1995): Vehicle Body Structure Durability Analysis. *SAE Technical Paper* No. 951096.

Kuo, E.Y., and S. G. Kelkar. 1995. Body Structure Durability Analysis. *Automotive Engineering*, vol. 103, no. 7, pp. 73-77.

Lipton, C.; Juvinall, R.C. (1963): *Handbook of stress and strength- Design and Materials Application*. Macmillan & Co., New York, USA.

Manson, S.S. (1953): Behaviour of Materials under Conditions of Thermal Stress. *Heat Transfer Symposium, University of Michigan Engineering Research Institute*, pp. 9-75.

Matsuishi, M.; Endo T. (1968): Fatigue of Metals Subjected to Varying Stress. *Presented to JSME*, Fukuoko, Japan.

Miner, M.A. (1945): Cumulative Damage in Fatigue. *Journal of Applied Mechanics*, vol. 12, pp. 159-164.

Morrow, J. (1968): *Fatigue Design Handbook: Advances in Engineering*. Warrendale, PA: SAE, pp. 21-29.

Palmgren A. (1924): Durability of Ball Bearings. *ZVDI*, vol. 68, no. 14, pp. 339-341.

Schaeffer, H.G. (2001): *MSC.Nastran primer for static Analysis*, USA: MSC.Software Corporation.

Smith, K. N.; Watson, P.; Topper, T.H. (1970): A stress-strain functions for the fatigue on materials. *Journal of Materials*, vol. 5, no. 4, pp. 767-78.

Stephens, R.I.; Fatemi, A.; Stephens, R.R.; Fuchs, H.O. (2001): *Metal Fatigue in Engineering*. USA: John Wiley and Sons, Inc.

Tucker, L.; Bussa, S. (1997): The SAE Cumulative Fatigue Damage Test Program: Fatigue under Complex Loading. *SAE Technical Paper*, pp. 3-14.

Van Blarigan, P. (1998): Advanced Hydrogen Fueled Internal Combustion Engines. *Energy and Fuels*, vol. 12, pp. 72-77.

Wöhler, A. (1867). Wöhlers Experiment on the Strength of Metals. *Engineering*, vol. 4, pp. 160-161.

Yim, H.J.; Lee, S.B. (1996): An Integrated CAE System for Dynamic Stress and Fatigue Life Prediction of Mechanical Systems. *KSME International Journal*, vol. 10, no. 2, pp. 158-168.

